JOURNAL OF GUIDANCE, CONTROL, AND DYNAMICS
Vol. 29, No. 3, May–June 2006

Restructurable Guidance and Control for Aircraft with Failures Considering Gust Effects

Naoki Tanaka* and Shinji Suzuki†
University of Tokyo, Tokyo 113-8656, Japan
and
Kazuya Masui‡ and Hiroshi Tomita§
Japan Aerospace Exploration Agency, Tokyo 181-0015, Japan

This paper presents a procedure for designing a fault-tolerant guidance and control system for a damaged aircraft using the simultaneous online fault/wind estimation and the nonlinear restructurable guidance and control law. The algorithm employs an extended Kalman filter (EKF) and a nonlinear inverse dynamics (NID) controller with the singular perturbation method. The EKF, which is based on the six-degree-of-freedom nonlinear aircraft equations of motion, simultaneously estimates the aerodynamic derivative changes and the wind-velocity components. The NID controller computes the required control-surface deflections and engine thrust not only to stabilize damaged aircraft but also to enable the aircraft to track the reference trajectory using the estimated results in a gusty environment. The estimation algorithm is evaluated through flight-test data obtained by using the experimental aircraft. Numerical simulations are carried out to verify the guidance and control capability of damaged aircraft under gusty conditions.

Nomenclature

b	=	wing span
C	=	aerodynamic derivatives
$\bar{c}$	=	mean aerodynamic chord
D	=	total drag
F_t	=	linearized transition matrix
F_X, F_Y, F_Z	=	guidance forces about the moving axis along the flight path
f, g	=	nonlinear functions of state equations
g	=	acceleration of gravity
H_t	=	linearized output matrix
h	=	nonlinear function of output equations
I_6	=	six-dimensional identity matrix
K	=	guidance and control gains
K_t	=	Kalman gain
L	=	total lift
$\bar{L}, \bar{M}, \bar{N}$	=	aerodynamic moment components
l_e	=	engine moment arm
m	=	aircraft mass
$P_{t/t}, P_{t+1/t}$	=	estimation/prediction covariance
p, q, r	=	angular velocity components about the body axes
Q_t	=	process noise covariance
q_t	=	dynamic pressure
R_t	=	measurement noise covariance
S	=	wing area
T	=	thrust
t	=	time
u	=	input
V	=	velocity
v_t	=	measurement noise
W_X, W_Y, W_Z	=	wind-velocity components about earth fixed frame
w_t	=	process noise
X, Y, Z	=	position of aircraft
x	=	state
Y	=	side force
y	=	output
α	=	angle of attack
β	=	sideslip angle
γ	=	flight-path angle
$\delta_a, \delta_e, \delta_r$	=	surface deflections of aileron, elevator, and rudder
δ_{Th}	=	differential thrust
λ	=	heading angle
ξ	=	wind-velocity vector
ρ	=	air density
ϕ, θ, ψ	=	Euler angles

Subscripts

a	=	airspeed
c	=	reference
d	=	aerodynamic derivative
L/R	=	left/right

Superscripts

T	=	transpose
$(\dot{*})$	=	time derivative
$\wedge$	=	estimated value
$-$	=	mean value

Received 23 January 2005; revision received 31 October 2005; accepted for publication 1 November 2005.

*Graduate Student, Department of Aeronautics and Astronautics, 7-3-1 Hongo, Bunkyo-ku.

†Professor, Department of Aeronautics and Astronautics, 7-3-1 Hongo, Bunkyo-ku. Senior Member AIAA.

‡Team Leader, Airplane Section, Flight Systems Technology Center, 6-13-1 Osawa, Mitaka-shi.

§Associate Senior Researcher, Airplane Section, Flight Systems Technology Center, 6-13-1 Osawa, Mitaka-shi.

I. Introduction

RESTRUCTURABLE flight control systems have been investigated to improve the survivability of damaged aircraft. There are two basic approaches. The first is the fault detection and isolation (FDI)-based approach, which displayed its effectiveness in the flight testing of the so-called self-repairing flight control system.[1] Because the FDI approach requires prior assumptions regarding the characteristics of failures, adaptive control has been applied as the second approach without the use of the FDI process.[2] Furthermore,

the adaptive control approach is categorized into two methods—an indirect adaptive-control-based method and a direct adaptive-control-based method. NASA's Intelligent Flight Control System program[3] has been testing several flight control systems based on a neural network. The primary focus of this paper is the integration of the restructurable flight control and guidance algorithm for damaged aircraft in gusty conditions.

Although the effect of gusts or wind has not been considered seriously in research on restructurable control systems, wind or gusts influence aircraft dynamics. Lower frequency wind influences tracking performance for a specified flight path, and higher frequency wind or gusts affect flight stability characteristics. Although there are many approaches to both online parameter identification[4] and restructurable flight control,[2] to incorporate wind effects, this paper adopts the extended Kalman filter (EKF) method[5] and the nonlinear inverse dynamics (NID) method.[6–10] Consequently, this paper employs an adaptive control approach based on an indirect method that identifies time-varying system parameters and uses those parameters to rebuild the flight control systems. Because a sudden change in flight characteristics due to any damage may result in a large movement with nonlinear behavior, the nonlinear dynamic equations should be considered for identification and control. Additionally, the singular perturbation method, which separates the system dynamics into several submodels on the basis of a time scale, can enhance robust characteristics to feedforward terms in NID.[7,8]

To consider the wind effect in the design of a restructurable control system, wind components must be estimated in the parameter identification process. Because a low-altitude wind may pose a significant hazard to a low-speed flight such as take off or landing, problems regarding the identification of wind-velocity components have been investigated in previous research.[11,12] Reference 12 applied the EKF to identify the wind components that are used to decide the control strategy in an NID control architecture. This study applies a similar approach to the restructurable flight control and guidance problems. Both the aerodynamic derivatives and the wind-velocity components are identified using the EKF method. The obtained information is used to reconstruct an NID control module that has the capability to control damaged aircraft and guide a specified flight path by canceling wind forces. It should be mentioned that some fundamental assumptions are made in our study: 1) all the states of the motion equations can be measured without any sensor failure, 2) failure is modeled as a change in aerodynamic derivatives, 3) the closed-loop system is stable even after failures, and 4) both observability and controllability are guaranteed even after failures. If there is complete loss of a control surface, an additional control device should be introduced to ensure the assumptions noted above. In numerical simulations, a differential thrust operation[13] is employed to compensate for the loss of rudder effectiveness. Although our approach is considered to be practical, mathematical verification of stability bounds is difficult. Hence, no stability analysis was performed in this study.

In Section II, the dynamic equations including wind effects are explained briefly, and in the subsequent Sections III and IV, the estimation and control algorithms are described. The estimation algorithm is verified in Section V, where the flight experiment vehicle[14] of the Japan Aerospace Exploration Agency is used to compare the estimated wind velocities with the measurement data. It also notes that some stability derivatives are estimated simultaneously. In Section VI, the integration of the parameter estimation and the restructurable control system is evaluated by numerical simulations. Two cases, aileron reversal and vertical fin loss, are considered. Although our approach can take into account the changes in a time-varying system, it is assumed that the aerodynamic derivatives change suddenly at failure. Both the transient characteristics and the tracking performance will be evaluated in these simulations. Finally, in Section VII, the summary and conclusions of this paper are presented.

II. Aircraft Dynamics and Failure Model

A. Aircraft Gust Response Model

A nonlinear six-degree-of-freedom model of an aircraft with gusts effect is used in this study.[15] This aircraft has traditional aerodynamic control surfaces, that is, elevator for pitch control, ailerons for roll control, and rudder for yaw control. The nonlinear continuous aircraft equations of motion with gusts terms can be expressed as

$$\dot{x} = f(x, u, \xi), \qquad y = h(x, u, \xi) \tag{1}$$

where $x = [V_a \;\; \alpha_a \;\; \beta_a \;\; \phi \;\; \theta \;\; \psi \;\; p \;\; q \;\; r]^T$ represents the aircraft state vector, $u = [T \;\; \delta_a \;\; \delta_e \;\; \delta_r]^T$ represents the control input vector, and $\xi = [W_X \;\; W_Y \;\; W_Z]^T$ represents the wind velocity vector.

The aerodynamic forces and moments are expressed as follows:

$$D = q_t S C_D, \qquad L = q_t S C_L, \qquad Y = q_t S C_Y$$

$$\bar{L} = q_t S b C_l, \qquad \bar{M} = q_t S \bar{c} C_m, \qquad \bar{N} = q_t S b C_n \tag{2}$$

Further, the aerodynamic derivatives are expanded as a linear combination of the state values as follows:

$$C_D = C_{D0}, \qquad C_L = C_{L\alpha}\alpha_a + C_{Lq}\bar{c}q/(2V_a), \qquad C_Y = C_{Y\beta}\beta_a$$

$$C_l = C_{l\beta}\beta_a + C_{lp}bp/(2V_a) + C_{lr}br/(2V_a) + C_{l\delta_a}\delta_a + C_{l\delta_r}\delta_r$$

$$C_m = C_{m0} + C_{m\alpha}\alpha_a + C_{m\dot{\alpha}}\bar{c}\dot{\alpha}/(2V_a) + C_{mq}\bar{c}q/(2V_a) + C_{m\delta_e}\delta_e$$

$$C_n = C_{n\beta}\beta_a + C_{np}bp/(2V_a) + C_{nr}br/(2V_a) + C_{n\delta_a}\delta_a + C_{n\delta_r}\delta_r \tag{3}$$

B. Failure Cases

Failures can be modeled as changes in the aerodynamic derivatives and detected by comparing nominal values with estimated data. In this paper, the following failures are considered and no sensor failures are assumed:

1) *Control Surface Failure:* Loss of effectiveness of a control surface is considered. In this case, the aerodynamic derivatives will change according to the type of control-surface failure.

2) *Aerodynamic Shape Change:* The aerodynamic shape of an aircraft changes when some of its parts are lost. For example, if the aircraft loses part of or the entire vertical fin, the directional stability, spiral performance, and rudder effectiveness will worsen. In such a situation, the aerodynamic derivatives, which are functions of the vertical fin shape, will change.

III. Fault Detection and Isolation and Wind Estimation

To estimate the aerodynamic derivatives and wind-velocity components, the EKF method is applied. It is considered that the EKF is suitable for parameter identification of damaged aircraft because it does not assume that the system is linear, stable, or time-invariant.

The EKF computes minimum variance estimates for nonlinear systems described by the equations

$$x_{t+1} = f_t(x_t) + w_t, \qquad y_t = h_t(x_t) + v_t \tag{4}$$

The filter equations are

$$\hat{x}_{t+1/t} = f_t(\hat{x}_{t/t}), \qquad \hat{x}_{t/t} = \hat{x}_{t/t-1} + K_t[y_t - h_t(\hat{x}_{t/t-1})] \tag{5}$$

The Kalman gain is

$$K_t = P_{t/t-1}H_t^T\left[H_t P_{t/t-1} H_t^T + R_t\right]^{-1} \tag{6}$$

The covariance equations are

$$P_{t+1/t} = F_t P_{t/t} F_t^T + Q_t$$

$$P_{t/t} = P_{t/t-1} - P_{t/t-1}H_t^T\left[H_t P_{t/t-1} H_t^T + R_t\right]^{-1} H_t P_{t/t-1} \tag{7}$$

The initial values are

$$\hat{x}_{0/-1} = \bar{x}_0, \qquad P_{0/-1} = \Sigma_0 \tag{8}$$

where

$$F_t = \left(\frac{\partial f_t}{\partial x_t}\right)_{x=\hat{x}_{t/t}}, \qquad H_t = \left(\frac{\partial h_t}{\partial x_t}\right)_{x=\hat{x}_{t/t-1}} \tag{9}$$

Then, the dynamic model for the EKF is constructed. The wind-velocity dynamics is expressed as

$$\dot{x}_g = W x_g, \qquad W = \begin{bmatrix} 0 & I_6 \\ 0 & 0 \end{bmatrix} \tag{10}$$

where $x_g = [\xi \;\; \dot{\xi} \;\; \ddot{\xi}]^T$. Equation (10) represents the integral state model.[16] It is assumed that the dynamics of the third time derivatives of ξ is much slower than the sampling rate and it is therefore neglected. Similarly, failure dynamics is not considered. Therefore, the combined aircraft/wind/failure dynamics is expressed as

$$x_{ex} = \begin{bmatrix} x^T & x_g^T & x_d^T \end{bmatrix}^T, \qquad \dot{x}_{ex} = \begin{bmatrix} f(x_{ex}, u) \\ W x_g \\ 0 \end{bmatrix} + w_t$$

$$y = h(x_{ex}, u) + v_t \tag{11}$$

where $x_d = [C_{l\delta_a} \;\; C_{m\delta_e} \;\; C_{n\delta_r} \;\; \cdots]^T$ is the vector of the aerodynamic derivatives to be estimated. Equation (11) describes the system model that is assumed to design the EKF. The unknown aerodynamic derivatives and wind-velocity components are added to the state elements. This implies that the parameter identification and disturbance estimation problem is transformed into a state estimation problem. Then the EKF based on Eq. (11) outputs the aircraft state, aerodynamic derivatives, and wind-velocity components. The estimation algorithm is summarized as follows

1) Choose the aerodynamic derivatives that will change based on the failure.
2) Describe the combined aircraft/wind/failure model.
3) Design the extended Kalman filter.
4) Estimate the unknown aerodynamic derivatives and wind-velocity components.
5) Apply the estimated data for guidance and control.

IV. Restructurable Control

The NID guidance and control law is employed for tracking a given flight path and for controller reconstruction.

The system is represented as

$$\dot{x} = f(x) + g(x)u, \qquad y = h(x, u) \tag{12}$$

It is possible to construct a nonlinear feedback control law that provides output decoupling of y or its derivatives such that $y^{(d)} = v$, where d is the relative degree of differentiation required to identify the direct control effect on each element of the output vector. The vector $y^{(d)}$ is expressed as

$$y^{(d)} = f^*(x) + g^*(x)u = v \tag{13}$$

The new control input v can be chosen to place the system poles in the desired locations. Then, the inverse control law is expressed as

$$u = [g^*(x)]^{-1}[v - f^*(x)] \tag{14}$$

The general NID control law requires that the nonlinear plant be minimum phase because the resulting control law effectively inverts the plant, and otherwise would produce a closed-loop system that was internally unstable. If the system can be partitioned into slow- and fast-time-scale subsystems, the controller can be simplified. The separation of the dynamics into slow and fast time scales is a natural consequence of the underlying physics. In this paper, it is assumed that the angular velocity of the aircraft increases at a greater rate than the altitude and velocity. Then the singular perturbation method (SPM) can be applied to simplify the controller, and it improves the controller's robustness.

Next, the guidance controller design procedure is explained. First, the guidance force is computed from the reference flight path, the velocity, and the position of the aircraft. The components about the moving axis along the flight path are[10]

$$\begin{aligned} F_X &= m[\dot{V}_c + K_V(V_c - V) + g\sin\gamma_c + K_X\{(X_c - X)\cos\lambda_c\cos\gamma_c\} \\ &\quad + (Y_c - Y)\sin\lambda_c\cos\gamma_c + (Z_c - Z)\sin\gamma_c] \\ F_Y &= m[V_c\dot{\lambda}_c\cos\gamma_c + V_c K_\lambda(\lambda_c - \lambda)\cos\gamma_c \\ &\quad - K_Y\{(X_c - X)\sin\lambda_c + (Y_c - Y)\cos\lambda_c\}] \\ F_Z &= m\{-V_c\dot{\gamma}_c - V_c K_\gamma(\gamma_c - \gamma) - g\cos\gamma_c \\ &\quad + K_Z[(X_c - X)\cos\lambda_c\sin\gamma_c] \\ &\quad + (Y_c - Y)\sin\lambda_c\sin\gamma_c + (Z_c - Z)\cos\gamma_c\} \end{aligned} \tag{15}$$

Second, the desired thrust, angle of attack, sideslip angle, and bank angle are computed from the required guidance force as follows:

$$\begin{aligned} T_c &= F_x + D, \qquad \alpha_c = (F_y\sin\phi_c - F_z\cos\phi_c)/q_t S C_{L\alpha} \\ \beta_c &= (F_y\cos\phi_c + F_z\sin\phi_c)/q_t S C_{Y\beta} \\ \phi_c &= \tan^{-1}(-F_y/F_z) \end{aligned} \tag{16}$$

Here, it is assumed that only the control surfaces produce the aerodynamic moment for stability. Otherwise, the open-loop system tends to be a nonminimum phase and the closed-loop system is unstable. This completes the computation for the guidance subsystem. Third, the desired angular velocities are computed using the inverse systems of the angle of attack, sideslip angle, and bank angle, which are termed slow-time-scale (STS) subsystems. The state equation of the STS is expressed as

$$\begin{bmatrix} \dot{\alpha} \\ \dot{\beta} \\ \dot{\phi} \end{bmatrix} = \begin{bmatrix} f_\alpha(x,\xi) \\ f_\beta(x,\xi) \\ f_\phi(x,\xi) \end{bmatrix} + \begin{bmatrix} g_{\alpha p}(x) & g_{\alpha q}(x) & g_{\alpha r}(x) \\ g_{\beta p}(x) & g_{\beta q}(x) & g_{\beta r}(x) \\ g_{\phi p}(x) & g_{\phi q}(x) & g_{\phi r}(x) \end{bmatrix} \begin{bmatrix} p \\ q \\ r \end{bmatrix} \tag{17}$$

Therefore, the NID control law is

$$\begin{bmatrix} p_c \\ q_c \\ r_c \end{bmatrix} = \begin{bmatrix} g_{\alpha p}(x) & g_{\alpha q}(x) & g_{\alpha r}(x) \\ g_{\beta p}(x) & g_{\beta q}(x) & g_{\beta r}(x) \\ g_{\phi p}(x) & g_{\phi q}(x) & g_{\phi r}(x) \end{bmatrix}^{-1} \begin{bmatrix} U_\alpha - f_\alpha(x,\xi) \\ U_\beta - f_\beta(x,\xi) \\ U_\phi - f_\phi(x,\xi) \end{bmatrix} \tag{18}$$

where

$$\begin{aligned} U_\alpha &= (K_{\alpha P} + K_{\alpha I}/s)(\alpha_c - \alpha_a) \\ U_\beta &= (K_{\beta P} + K_{\beta I}/s)(\beta_c - \beta_a) \\ U_\phi &= (K_{\phi P} + K_{\phi I}/s)(\phi_c - \phi) \end{aligned} \tag{19}$$

are the feedback control laws that enable α, β, ϕ to track the reference values $\alpha_c, \beta_c, \phi_c$. Finally, the required control surface deflections are computed using the inverse systems of angular velocities, which are termed fast-time-scale (FTS) subsystems. The state equation of the FTS is expressed as

$$\begin{bmatrix} \dot{p} \\ \dot{q} \\ \dot{r} \end{bmatrix} = \begin{bmatrix} f_p(x) \\ f_q(x) \\ f_r(x) \end{bmatrix} + \begin{bmatrix} g_{pa}(x) & 0 & g_{pr}(x) \\ 0 & g_{qe}(x) & 0 \\ g_{ra}(x) & 0 & g_{rr}(x) \end{bmatrix} \begin{bmatrix} \delta_a \\ \delta_e \\ \delta_r \end{bmatrix} \tag{20}$$

Therefore, the NID control law is

$$\begin{bmatrix} \delta_a \\ \delta_e \\ \delta_r \end{bmatrix} = \begin{bmatrix} g_{pa}(x) & 0 & g_{pr}(x) \\ 0 & g_{qe} & 0 \\ g_{ra}(x) & 0 & g_{rr}(x) \end{bmatrix}^{-1} \begin{bmatrix} U_p - f_p(x) \\ U_q - f_q(x) \\ U_r - f_r(x) \end{bmatrix} \tag{21}$$

where

$$U_p = K_p(p_c - p), \qquad U_q = K_q(q_c - q), \qquad U_r = K_r(r_c - r) \tag{22}$$

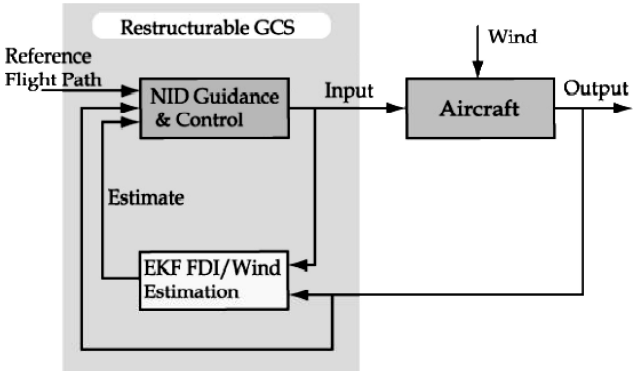

Fig. 1 Fault-tolerant guidance and control system.

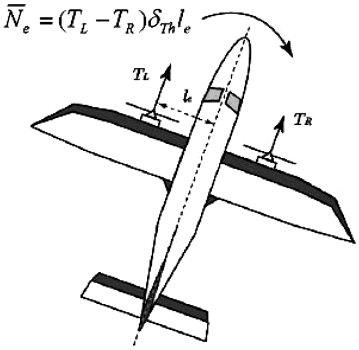

Fig. 2 Differential thrust at vertical fin loss.

are the feedback-control laws. It should be mentioned that the feedback-control gains must be designed to ensure closed-loop stability. When the effects of failures are estimated, the control parameters in the STS and FTS are updated and the effects of wind and gusts are eliminated using the estimated data. In other words, when the control devices (aileron, elevator, rudder, etc.) fail, g_{ij} are updated. When the aerodynamic shape changes due to accidents, f_i and g_{ij} are updated. The closed loop system is shown in Fig. 1.

This method requires that the closed-loop system be stable and the controllability be guaranteed even after failures. Therefore, for serious failures, the functions of the aircraft that are lost should be compensated for by the remaining control devices. Those functions will be considered in numerical simulations described in section VI. For example, when the rudder effectiveness is seriously hampered, the yawing cannot be controlled. In that case, differential thrust can be used.[13] That is, the desired yawing moment $\bar{N}_e$ is generated by the thrust difference between the left and the right engines, expressed as

$$\bar{N}_e = (T_L - T_R)\delta_{\mathrm{Th}} l_e \tag{23}$$

where l_e is the moment arm as shown in Fig. 2. The effect on the rolling and pitching moments is neglected. The equations of motion are modified as

$$\begin{bmatrix} \dot{p} \\ \dot{r} \end{bmatrix} = \begin{bmatrix} f_p(x) \\ f_r(x) \end{bmatrix} + \begin{bmatrix} g_{pa}(x) & g_{pt}(x) \\ g_{ra}(x) & g_{rt}(x) \end{bmatrix} \begin{bmatrix} \delta_a \\ \tilde{\delta}_{\mathrm{Th}} \end{bmatrix} \tag{24}$$

where $\tilde{\delta}_{\mathrm{Th}}$ is the ratio of δ_{Th} to $q_t S$. Thus, the desired aileron deflection and the thrust difference are calculated as follows:

$$\begin{bmatrix} \delta_a \\ \tilde{\delta}_{\mathrm{Th}} \end{bmatrix} = \begin{bmatrix} g_{pa}(x) & g_{pt}(x) \\ g_{ra}(x) & g_{rt}(x) \end{bmatrix}^{-1} \left(\begin{bmatrix} U_p \\ U_r \end{bmatrix} - \begin{bmatrix} f_p(x) \\ f_r(x) \end{bmatrix} \right) \tag{25}$$

Similarly, when the function of the elevator is lost, the longitudinal motion is compensated using the flaps, which function as the horizontal stabilizer. However, these types of controls are not used in normal operation, because the movements of these devices are slower than those of the control surfaces, and are basically unsuitable for altitude control. Further, when failure occurs, it is necessary to switch the control method. In this study, some threshold values of typical parameters have been provided, and the controller is switched based on the estimated data. For example, when the estimated rudder effectiveness ($C_{l\delta_r}$, $C_{n\delta_r}$) becomes smaller than the threshold, the controller is switched to use differential thrust instead of rudder.

V. Flight Test of Estimation Algorithm

The estimation algorithm presented in Section III is applied to flight experiment data to confirm the estimation algorithm. The flight was made on October 27, 2004. The Japan Aerospace Exploration Agency has developed a flight experiment vehicle, the Multi Purpose Aviation Laboratory-α (MuPAL-α).[14] This is a modified twin-turboprop aircraft, Dornier Do228-202. Numerical data on the aircraft are the following: mass $m = 5930$ kg, wing area $S = 32.0\ \mathrm{m}^2$, wing span $b = 16.97$ m, and mean aerodynamic chord $\bar{c} = 2.046$ m. The flight data was obtained using MuPAL-α, which can measure the aircraft state, control surface deflections, engine torque, and ground speed. The sensor data used for estimation were

$$y = \begin{bmatrix} x^T & \dot{V}_a & \dot{\alpha}_a & \dot{\beta}_a & \dot{p} & \dot{r} \end{bmatrix}^T, \qquad u = \begin{bmatrix} T & \delta_a & \delta_e & \delta_r \end{bmatrix}^T \tag{26}$$

The derivative of each state component is obtained by numerical differentiation. The measurement noise covariance R_t was determined from the sensor accuracy.[4] The process noise covariance Q_t must be specified before the online parameter estimation. The strength of the process noise influences the characteristics of the estimated wind velocities. Therefore, the stochastic characteristics of the wind velocities during the flight should be obtained beforehand.[11,12] In this research, the process noise covariance Q_t

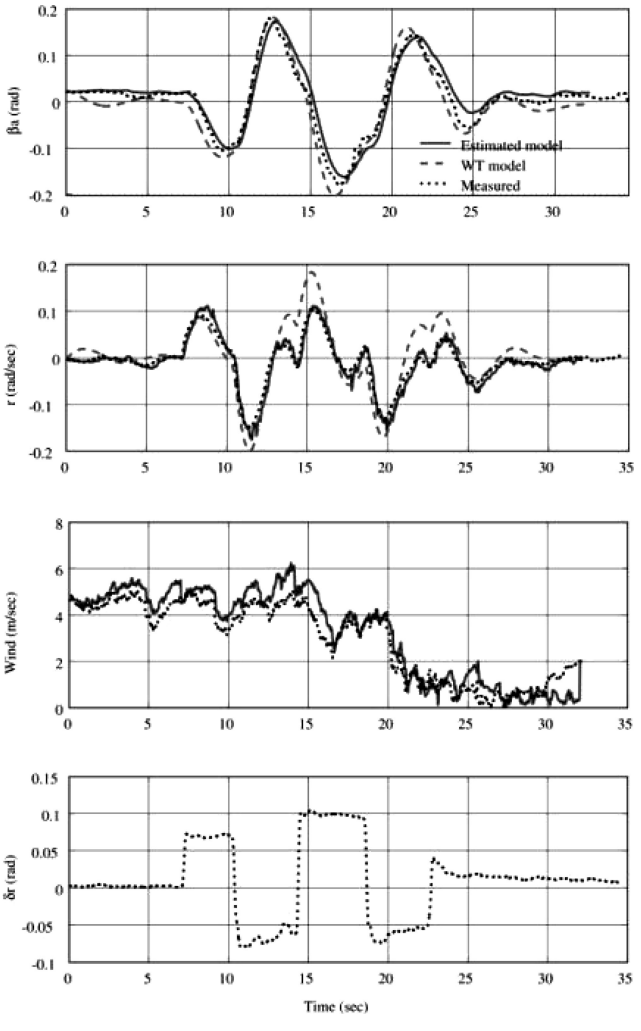

Fig. 3 Comparison of measured and estimated data (rudder input).

was adjusted by comparing the wind conditions and the estimated wind velocities. The average airspeed was approximately 65 m/s, and the altitude was about 5000 ft. The sampling rate was 50 Hz. No closed-loop controller was used in this flight test in order to obtain open-loop results. All flaps and landing gear were retracted, and the throttle was fixed. The lateral aerodynamic derivatives ($C_{Y\beta}$, $C_{l\beta}$, C_{lp}, C_{lr}, $C_{l\delta_a}$, $C_{n\beta}$, C_{np}, C_{nr}, $C_{n\delta_r}$) and the horizontal wind velocity were estimated. The derivatives whose effects appear to be small are fixed for the wind tunnel (WT) test data, such as $C_{l\delta_r}$, $C_{n\delta_a}$. Two test cases were prepared to evaluate performance of the estimation algorithm. The first case was the directional stability estimation, and the second case was the aileron effectiveness estimation.

Case 1: The estimation of the directional stability changes was tested. Two ventral fins were added to MuPAL-α, but only a single WT daturn was analyzed before modification. Therefore, the directional stability data did not appear to be accurate. The initial values of the aerodynamic derivatives were set to those of the WT data. The rudder doublet was input manually by the pilots, and the EKF estimated the actual values from the sensor outputs. It should be noted that an appropriate input must be applied in order to obtain estimation data with high accuracy. The estimated data were recorded 12 times. One of the results is shown in Fig. 3. In this figure, the model using estimated aerodynamic derivatives (estimated model), the model derived from WT (WT model), and the sensor outputs (measured) are shown by solid, dashed, and dotted lines, respectively. The estimated model could reproduce the actual motion more accurately than the WT model. It is evident that the estimated model is superior to the WT model, particularly in the case of the yaw rate response. Further, the magnitude of the estimated horizontal wind velocity and that of the measured one (deviation of the groundspeed and airspeed) are shown. It should be noted that this experimental aircraft can measure the airspeed components using α- and β-vanes; however, these devices are not available in most commercial airplanes. Furthermore, because the process noises and aircraft motion data should be estimated simultaneously, the measured wind velocities are not suitable for the proposed parameter estimation process. The estimated and measured wind velocities indicate good correlation.

Case 2: The aileron effectiveness was estimated. It is necessary that the correct parameters be estimated from the changed ones due to failures for FDI. However, it was difficult to conduct the experiment with aircraft that actually broke down. Therefore, to simulate the control surface loss, the initial value of the roll derivative against the aileron deflection $C_{l\delta_a}$ was intentionally set to a value much greater than that of the WT data (120, 150, and 200% of the nominal value). If a correct value is estimated from the initial incorrect value, it indicates that failures can be detected appropriately. The aileron-doublet maneuvers and coordinated turns were performed. The actual values were estimated by the EKF using sensor outputs. One of the results is shown in Fig. 4. This figure shows the time history of the state and data obtained from a coordinated-turn maneuver. In this figure, the initial value of $C_{l\delta_a}$ was set to 200% of the value of the WT data, but the estimated value converged to a realistic one. The converged value is very similar to that of the WT data. Therefore, it appears that the EKF can possibly estimate the actual aerodynamic derivatives when the aircraft loses control surfaces effectiveness. Furthermore, the estimated (solid) and measured (dotted) horizontal wind velocities were compared. The estimated and measured wind velocities indicate good coorelation.

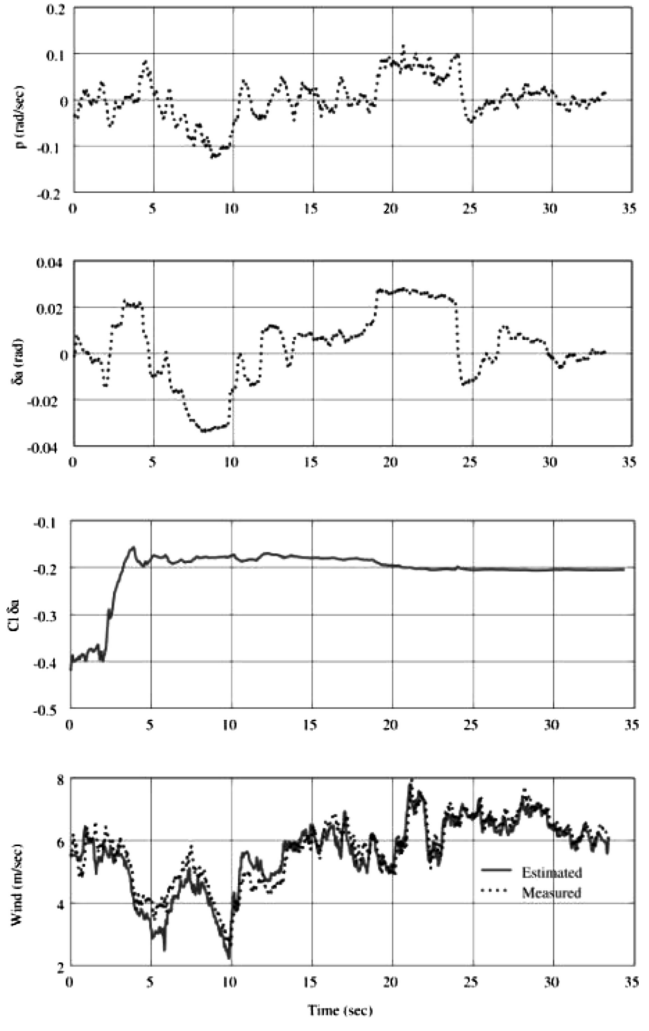

Fig. 4 Time histories of measured and estimated data (aileron input).

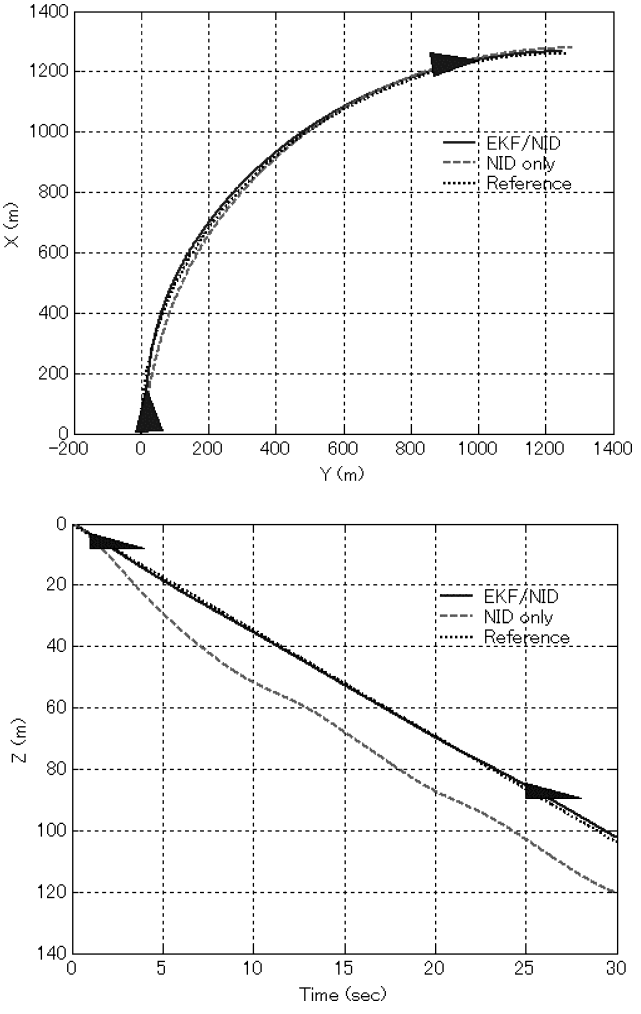

Fig. 5 Flight trajectories with gusts and without failure.

Because the EKF method is based on the linearlization of the system, it may be trapped in local minimums or it may become unstable, especially in highly nonlinear cases. Furthermore, the system must satisfy the condition of observability and be excited in an appropriate manner. Although the flight-test results show good performance by applying our approach, these items must be considered in parameter identification problems.

VI. Numerical Simulations

The algorithm is applied to aircraft guidance and control. Two numerical simulations are presented to demonstrate the performance of the proposed algorithm. The control objective is to enable a damaged aircraft to track the reference trajectory in a gustsy environment. The aircraft model is the same as that used in the previous section—MuPAL-α. An altitude of 5000 ft and a speed of 70 m/s are the initial conditions in the simulations. It is assumed that the engine thrust has first-order dynamics with a time constant of 1.0 s. In this flight condition, the control-surface position limits are

$$-10\,\text{deg} \le \delta_a \le 10\,\text{deg}, \qquad -10\,\text{deg} \le \delta_e \le 5\,\text{deg}$$

$$-10\,\text{deg} \le \delta_r \le 10\,\text{deg} \tag{27}$$

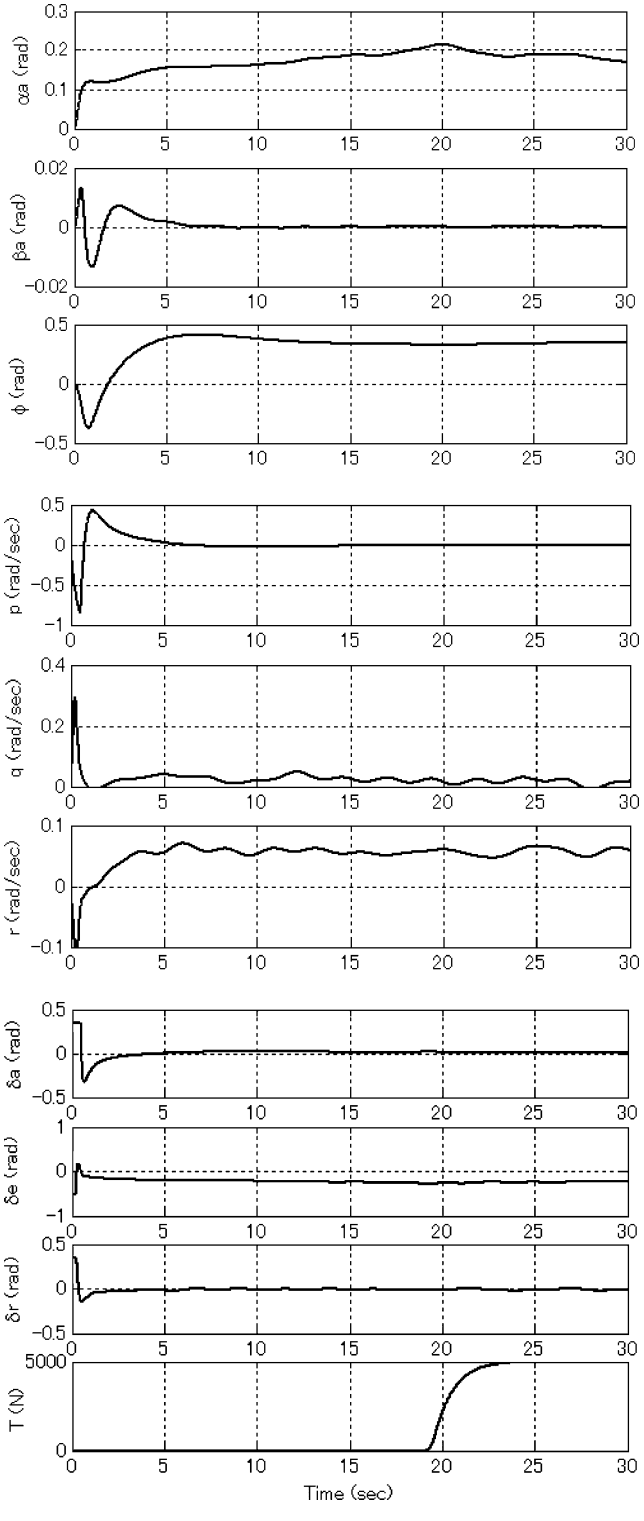

Fig. 6 Time responses with gusts and without failure (EKF/NID).

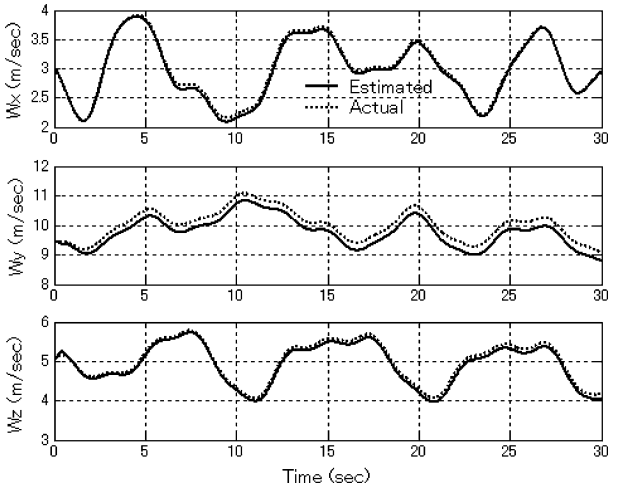

Fig. 7 Time histories of estimated wind velocities.

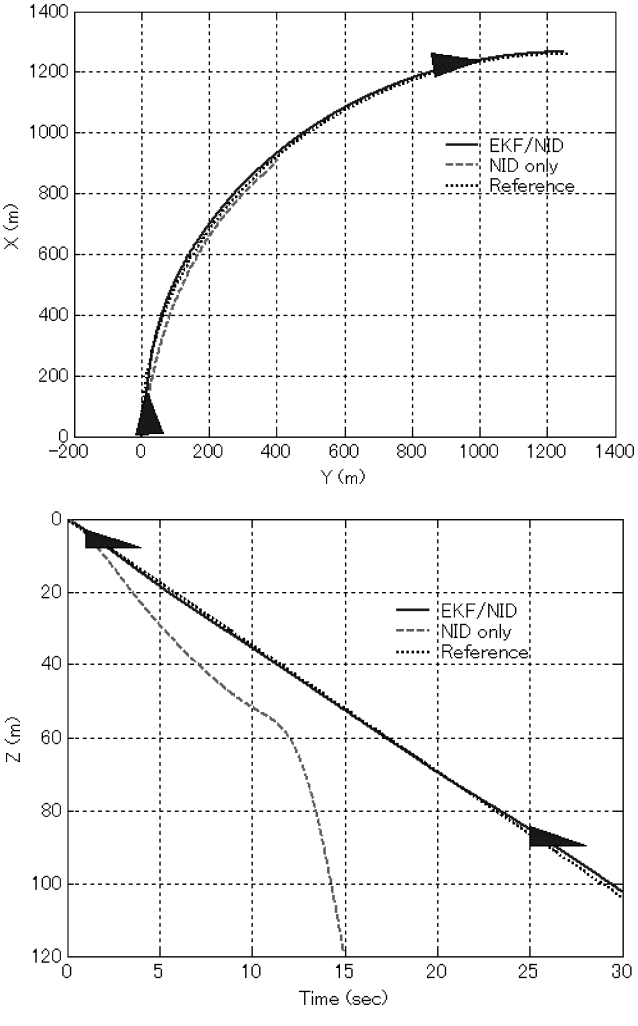

Fig. 8 Flight trajectories with aileron reversal and gusts.

The actuator dynamics are not included. The reference flight path simulates a landing approach with a turn. Controller gains (K_V, K_γ, K_λ, K_X, K_Y, K_Z, K_α, K_β, K_ϕ, K_p, K_q, K_r) are determined from the response of the nominal aircraft without failures in the absence of wind. It should be mentioned that the method combining parameter estimation with a nonlinear controller is practical; however, it is difficult to prove the stability and convergence criteria of the total system.[2] Therefore, controller gains should be selected to allow sufficient stability margin to the nominal system. The control performances EKF/NID are compared to those with NID alone. The sampling rate for the simulations is 50 Hz.

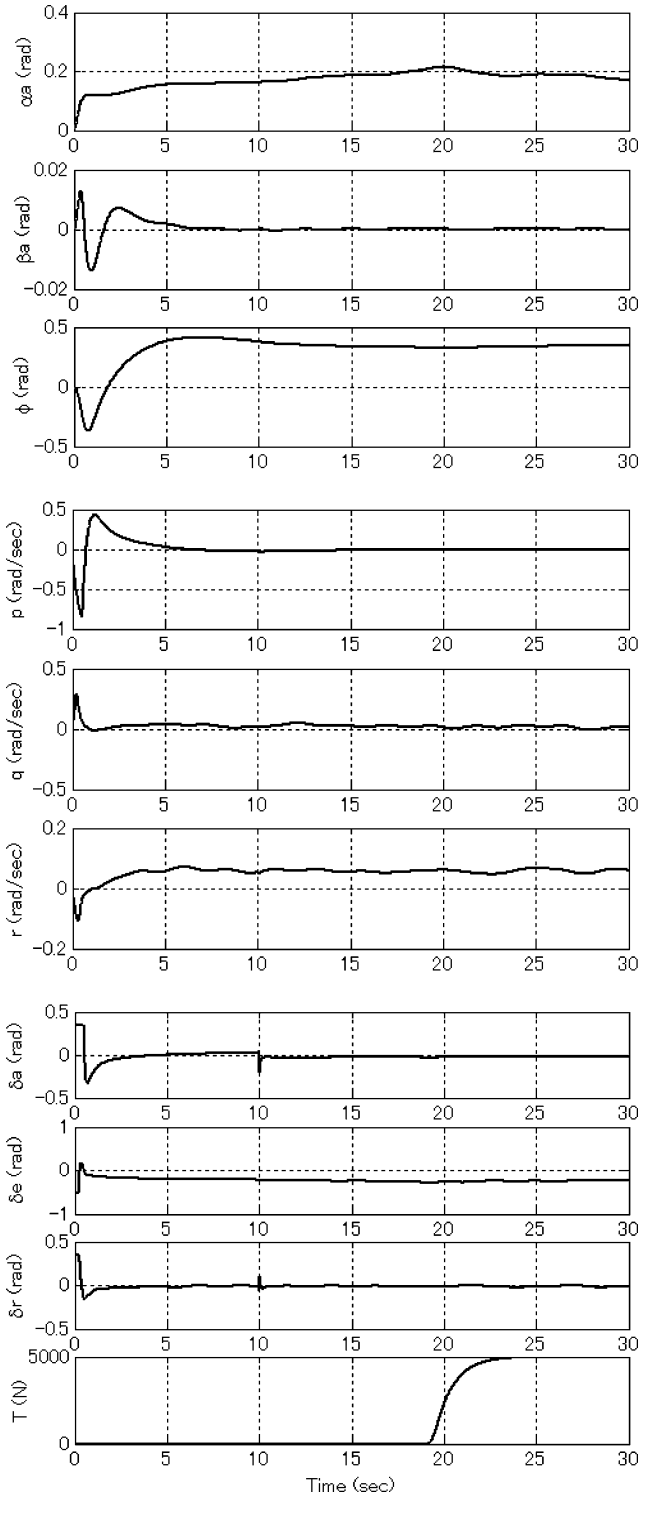

Fig. 9 Time responses with aileron reversal and gusts (EKF/NID).

Initially, wind effects are considered. No failure occurs. The flight trajectories are shown in Fig. 5. Time responses and estimated wind velocities are shown in Figs. 6 and 7. It is obvious that tracking performance is improved by utilizing the estimated wind velocity. The maximum tracking error of heights is approximately 1 m (with EKF/NID) and 18 m (without EKF). In the lateral directions, the maximum tracking errors are approximately 8 m (with EKF/NID) and 40 m (without EKF). The state response and control input are stable and reasonable, the wind velocity is successfully estimated by EKF, and the estimated data is utilized to track the flight path with high accuracy.

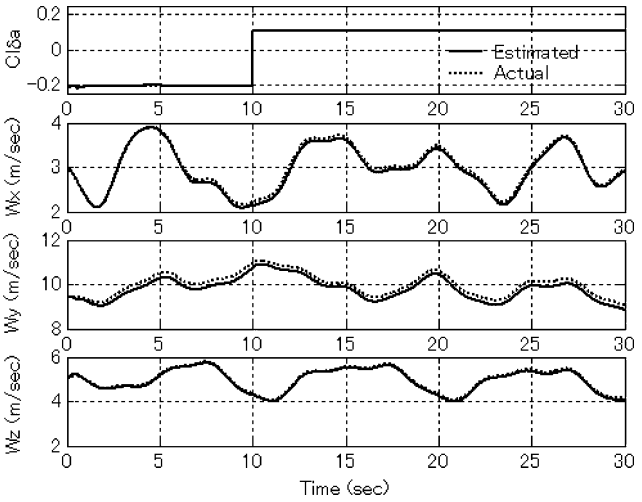

Fig. 10 Time histories of estimated $C_{l\delta_a}$ and wind velocities with aileron reversal.

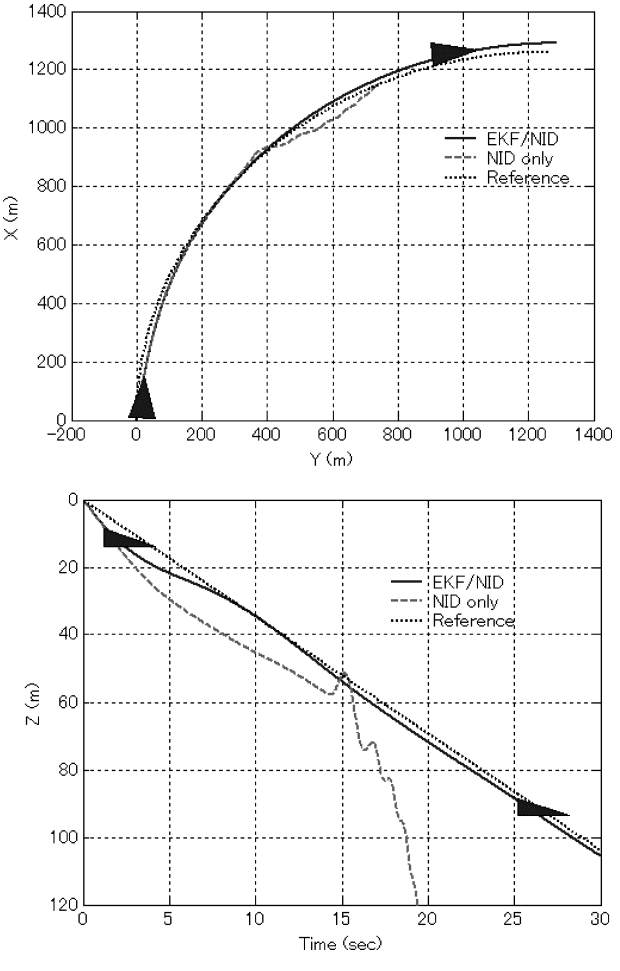

Fig. 11 Flight trajectories with vertical fin loss and gusts.

As the next step, two failure cases are simulated as follows.

Scenario 1: The aileron effectiveness becomes reversed (aileron reversal). Although there are some causes that lead to aileron reversal, it is assumed that the roll derivative against the aileron deflection $C_{l\delta_a}$ reverses suddenly, as the worst-case scenario. The accident occurs at $t = 10.0$ s. The flight trajectories are compared in Fig. 8. Time responses and the data of the aircraft estimated by EKF/NID are shown in Figs. 9 and 10, where the EKF accurately estimates the changed aerodynamic derivatives corresponding to the aileron deflections and wind velocity. The NID is updated using the estimated data, and the aircraft successfully tracks the reference trajectory. When the failure occurs at $t = 10.0$ s, it is observed that the control surfaces move rapidly. However, the magnitude of the changes is not significant and the transition of states is stable and smooth. In contrast, it is difficult for the aircraft with only the NID controller and without controller reconstruction to continue flight, because the NID controller cannot take into account the change in the stability derivative.

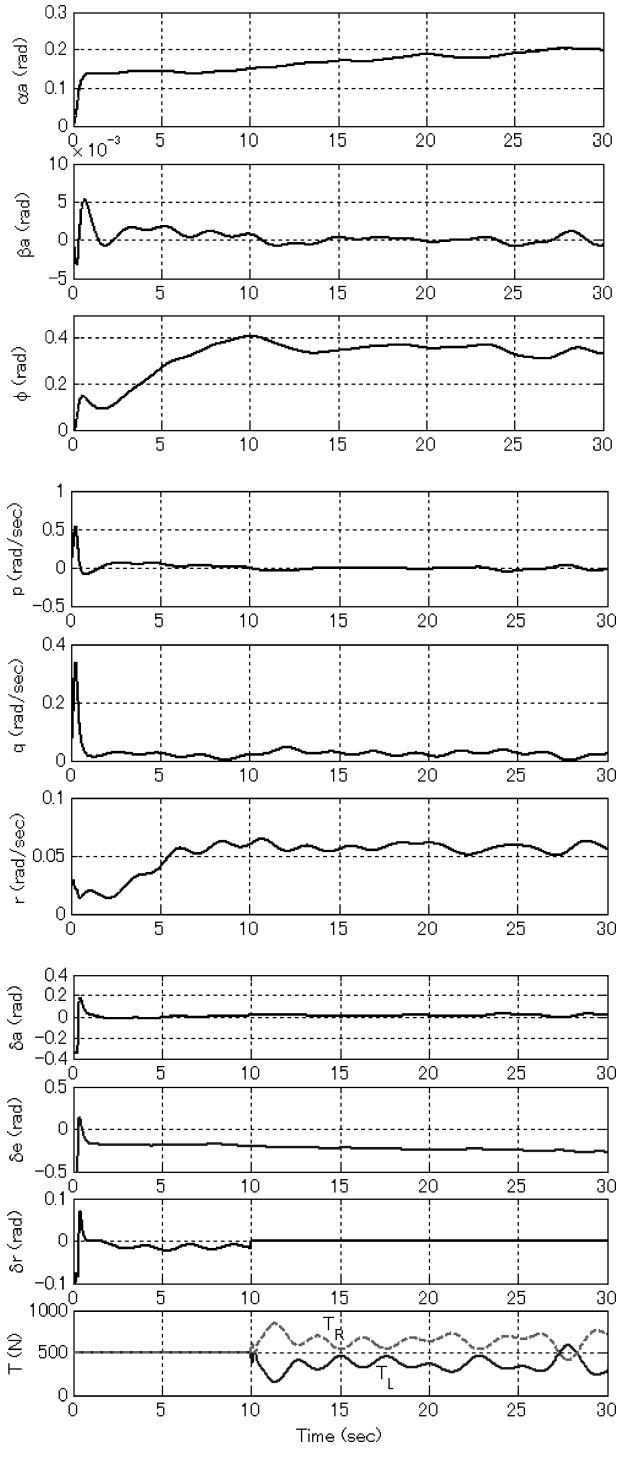

Fig. 12 Time responses with vertical fin loss and gusts (EKF/NID).

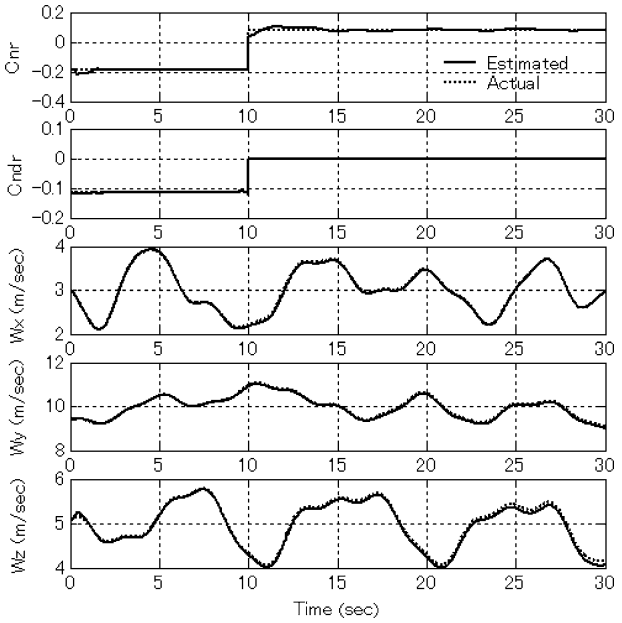

Fig. 13 Time histories of estimated C_{nr} and $C_{n\delta r}$ and wind velocities with vertical fin loss.

Scenario 2: The vertical fin is completely lost. The accident occurs at $t = 10.0$ s. When the aircraft loses the vertical fin, the directional stability is almost lost and the rudder cannot be used. In such a case, the aerodynamic derivatives that are functions of the vertical fin shape $C_{Y\beta}$, $C_{n\beta}$, C_{lr}, C_{nr}, $C_{l\delta_r}$, $C_{n\delta_r}$ change. Therefore, if the estimated aerodynamic derivatives have abnormal values, the controller is switched to output the required differential thrust instead of the rudder deflections. The introduction of new control devices is necessary to ensure the closed-loop stability and maintain controllability of the system. The flight trajectories are compared in Fig. 11. The time responses and the data of the aircraft estimated by EKF/NID are shown in Figs. 12 and 13. Figure 13 illustrates that the sign of the yaw damping derivative C_{nr} changes and the control derivative $C_{n\delta r}$ becomes zero at $t = 10.0$ s when the aircraft loses the vertical fin. This indicates that the aircraft loses the directional stability and the control power of the rudder. Figure 13 also indicates that these changes in the aerodynamic derivatives illustrated by dotted lines are successfully estimated by the EKF. After the EKF can detect the loss of the vertical fin by estimating the associated aerodynamic derivatives, the controller is switched to the differential thrust control immediately (approximately 0.04 s later). Figure 12 shows that the rudder input becomes zero and the differential thrust is activated after the failure occurs. It is observed that the differential thrust is oscillatory because there is a time delay in the thrust change. However, the divergence in the transient motion does not occur as shown in Fig. 12. Figure 11 illustrates that the damaged aircraft can track the reference trajectory with EKF/NID, which estimates both the change in aerodynamic derivatives and the wind velocities and uses these changes to reconstruct the control system. On the other hand, the aircraft cannot continue to track with only the original NID controller, as shown in Fig. 11.

VII. Conclusions

A restructurable flight-control and guidance system for damaged aircraft under gustsy conditions has been investigated. The extended Kalman filter method can simultaneously identify both aerodynamic derivatives and wind component velocities. The changes in the aerodynamic derivatives are used to detect aircraft failures and reconstruct the nonlinear dynamic inversion control module that also uses the estimated wind velocities to improve the tracking performance

for a specified flight path. The parameter identification method is verified using the flight-test data. The estimated wind velocities show a good correlation with measured data obtained by the experimental aircraft equipped with special sensors, and the estimated aerodynamic derivatives indicate reasonable values. Two failure cases—the aileron reverse case and the total loss of vertical fin case—are simulated using differential thrust. While the problems are simplified, that is, all the states can be measured without sensor failure and failures are modeled as the sudden change in aerodynamic derivatives, the simulation results indicate the effectiveness of the proposed method. For future study, more realistic failure models should be investigated for multiple flight cases across the flight envelope.

References

[1]Urnes, J., Yearger, R., and Stewart, J., "Flight Demonstration of the Self-Repairing Flight Control System in a NASA F-15 Aircraft," National Aerospace Electronics Conf., Rept. 90CH2881-1, Dayton, OH, May 1990.

[2]Steinberg, M. L., "Comparison of Intelligent, Adaptive, and Nonlinear Flight Control Laws," *Journal of Guidance, Control, and Dynamics*, Vol. 24, No. 4, 2001, pp. 693–699.

[3]Urnes, J., Davidson, R., and Jacobson, S., "A Damage Adaptive Flight Control System Using Neural Network Technology," *Proceedings of the American Control Conference*, American Automatic Control Council, Dayton, OH, 2001, pp. 2907–2912.

[4]Jategaonkar, R. V., and Plaetschke, E., "Algorithm for Aircraft Parameter Estimation Accounting for Process and Measurement Noise," *Journal of Aircraft*, Vol. 26, No. 4, 1989, pp. 360–372.

[5]Stengel, R. F., *Stochastic Optimal Control: Theory and Application*, Wiley, New York, 1986, Chap. 4.

[6]Lane, S. H., and Stengel, R. F., "Flight Control Design Using Non-linear Inverse Dynamics," *Automatica*, Vol. 24, No. 4, 1988, pp. 471–483.

[7]Snell, S. A., Enns, D. F., and Garrard, W. L., "Nonlinear Inversion Flight Control for a Supermaneuverable Aircraft," *Journal of Guidance, Control, and Dynamics*, Vol. 15, No. 4, 1992, pp. 976–984.

[8]Azam, M., and Singh, N. S., "Invertibility and Trajectory Control for Nonlinear Maneuvers of Aircraft," *Journal of Guidance, Control, and Dynamics*, Vol. 17, No. 1, 1994, pp. 192–200.

[9]Sun, X. D., Woodgate, K. G., and Allwright, J. C., "Nonlinear Inverse Dynamics Control of Aircraft Using Spoilers," *Journal of Guidance, Control, and Dynamics*, Vol. 19, No. 2, 1996, pp. 475–482.

[10]Yonezu, Y., Dohi, N., Baba, Y., and Takano, H., "Trajectory Guidance and Control for an Aircraft," *Proceedings of the JSASS 17th International Session in 41st Aircraft Symposium*, Japan Society for Aeronautical and Space Sciences, Tokyo, 2003, pp. 161–164.

[11]Mulgund, S. S., and Stengel, R. F., "Aircraft Flight Control in Wind Shear Using Sequential Dynamic Inversion," *Journal of Guidance, Control, and Dynamics*, Vol. 18, No. 5, 1995, pp. 1084–1091.

[12]Mulgund, S. S., and Stengel, R. F., "Optimal Nonlinear Estimation for Aircraft Flight Control in Wind Shear," *Automatica*, Vol. 32, No. 1, 1996, pp. 3–13.

[13]Burken, J. J., and Burcham, F. W., Jr., "Flight-Test Results of Propulsion-Only Emergency Control System on MD-11 Airplane," *Journal of Guidance, Control, and Dynamics*, Vol. 20, No. 5, 1997, pp. 980–987.

[14]Masui, K., and Tsukano, Y., "Development of a New In-Flight Simulator MuPAL-α," *Proceedings of the AIAA Modeling and Simulation Technologies Conference and Exhibit*, AIAA, Reston, VA, 2000, pp. 14–17.

[15]Frost, W., and Bowles, R. L., "Wind Shear Terms in the Equations of Aircraft Motion," *Journal of Aircraft*, Vol. 21, No. 11, 1984, pp. 866–872.

[16]Bossi, J. A., and Bryson, A. E., Jr., "Disturbance Estimation for a STOL Transport During Landing," *Journal of Guidance, Control, and Dynamics*, Vol. 5, No. 3, 1982, pp. 258–262.